J. of Thermal Science Vol.10, No.3

Experimental Study on Melting in a Rectangular Enclosure Heated Below with Discrete Heat Sources

Zhou Jianhua [1] **Chen Zhongqi** [2] **Liu Dengying** [1] **Li Ji** [1]

1. Institute of Engineering Thermophysics, Chinese Academy of Sciences, Beijng 100080, China
2. Energy and Power Engineering School, Xi'an Jiaotong University, Xi'an 710049, China

The melting process of n-octadecane in a rectangular cavity with three discrete protruding heat sources on its bottom surface was studied experimentally. It was observed that the experimental process, for the geometric arrangement in this paper, is neither a fixed melting nor a contact melting, but one in which fixed melting and contact melting take place alternatively. The effects of Stefan number, initial subcooling and aspect ratio on the melting process are reported. The larger the Stefan number, the more frequently the contact melting may occur, so does the aspect ratio. The initial subcooling plays a role only in early stage. As the melting process proceeds, its effect on the melting process becomes less.

Keywords: solid-liquid phase change, rectangular cavity, fixed melting, contact melting, discrete heat sources.

Introduction

Solid-liquid phase change heat transfer involving melting and solidification has received considerable attention for many years because of its wide-ranging applications[1]. Generally speaking, there are two kinds of melting phenomena: fixed melting[2,3] and contact melting[4,5]. In the case of fixed melting, the solid phase change material is forced to remain stationary and the melted liquid takes up the space between the solid-liquid interface and the heat source surface. In the case of contact melting, the solid phase change material, or heat source, is free to move, or forced to move. Therefore, only a thin, liquid-filled gap exists between the solid-liquid interface and the heat source surface, and the melted liquid is forced to flow out of this gap. Thus, the heat transfer in contact melting can be enhanced greatly.

Because the solid-liquid phase change problems are nonlinear, their theoretical solutions are very difficult. So, some approximate analytical solutions have been presented[6-8]. Nevertheless, much of the emphasis has been put on experimental investigations[9-11] and numerical simulations[12,13]. Most of the work done in the past, however, has dealt with the melting of phase change material (PCM) from a whole heated wall with a constant temperature. Comparatively few studies have been reported on the melting process from discrete heat sources at a constant rate. The interest for this problem was evoked mainly by the cooling of electronic components. Increasing miniaturization and reduced spacing of chips on printed circuit boards require larger power dissipation, which cannot be met by conventional passive cooling techniques (such as natural air convection) alone. Under this circumstance, the use of PCMs is believed to be a promising alternative. One of the fundamental questions arise in this application is how to distribute the heat sources for a fixed amount of PCM so that the melting process is achieved in a given period of time while maintaining the heat sources at a moderate temperature.

The present paper described a preliminary experimental study on the melting process in a rectangular cavity heated below with discrete protruding sources. The surface temperatures of the heat sources were measured by thermocouples and the solid-liquid interface motion was recorded photographically.

Experimental Setup

The experimental system was shown in Fig.1. The beam from the He-Ne laser tube 1 traveled through a pinhole 2 and condenser 3, was then reflected by two mirrors 4 and 5, and eventually formed a parallel beam. This beam was passed through the test section 6 by properly aligning the mirrors 4 and 5. The screen 10 was a piece of frosted glass. The purpose of using frosted

Received 2000

Nomenclature

AR	aspect ratio, H_0/W	T	temperature, ℃
b	width of heat source, m	V	voltage; volume of liquid phase
C_p	specific heat, kJ/(kg·℃)	V_0	total volume of PCM
g	acceleration due to gravity, m/s^2	V/V_0	melt fraction
H_0	initial height of the PCM, m	W	width of the PCM
k	thermal conductivity, W/(m·℃)		**Greeks**
L	latent heat of fusion of the PCM, kJ/kg	α	thermal diffusivity, m^2/s
P	power, W	β	thermal coefficient of expansion, 1/℃
Pr	Prandtl number, ν/α	μ	dynamic viscosity, kg/(m·s)
q	heat flux, W/m^2	ν	kinematic viscosity, m^2/s
R	electrical resistance, Ω	ρ	density, kg/m^3
Ra	Rayleigh number, $g\beta(q\cdot 3b/k_l)H_0^3/(\nu\cdot\alpha)$		**Subscripts**
S_c	initial subcooling, $C_{pl}(T_m-T_i)/L$	i	initial state
Ste	Stefan number, $C_{pl}(q\cdot 3b/k_l)/L$	l	liquid phase
t	time, s	m	melting point
		s	solid phase

glass was to scatter the light so that it would not be directly incident on the camera lens and a better quality photograph could be obtained. The shape of the solid-liquid interface was recorded by a Nikon® camera 7. A highly sensitive thermostat 8, which can control the water temperature to within ±1/15℃, was used to supply water at a constant temperature. By circulating water from the thermostat in the multi-pass channel installed in the two vertical walls of the rectangular cavity, the temperature of the two sidewalls was maintained at a constant temperature slightly above the melting temperature of PCM, as proved to be necessary for achieving contact melting by a pretest. The wall temperature was measured by carefully calibrated thermocouples and recorded by using a data acquisition system 9. The output of the thermocouples was displayed on the screen of the digital voltmeter 11. A DC power supply unit 12 was used to power the discrete heater located at the bottom surface of the test section 6.

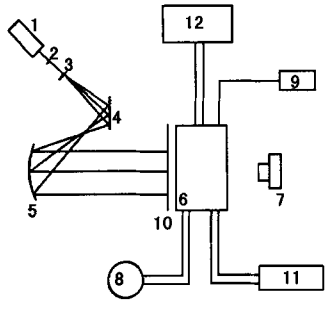

Fig.1 Experimental system

The melting experiments were performed in a rectangular cavity (Fig.2), whose inside dimensions were 100mm-height, 120 mm-width and 60mm-depth. The vertical heat exchanger 3 was made of copper. The top cover 1, auxiliary frame 2, vertical cover 4, horizontal inner wall 6, base 7, and flanges 10 and 11 were all made of Plexiglas. There were three discrete protruding heaters 5 on the horizontal inner wall 6. Three sheet heaters, which were made by wrapping constantan wire of 0.2mm diameter on a piece of bakelite of 0.5mm thick, were imbedded into these slots (60 mm×20 mm cross section with a depth of 4 mm) on the Plexiglas and then covered with mica and copper blocks of 11mm thick in order. So, each heat source 5 is 11-mm high, 20-mm wide and 60-mm long. The pitch of the discrete sheet heaters was 20 mm, heat-resistant adhesive was used to fix them in place, and the upper surface of the copper blocks was painstakingly hand-finished to ensure that they were in the same level. To minimize the heat loss from the back of the heaters, three auxiliary heaters 8 were mounted just opposite the main heaters and were maintained at the same temperature as the main heaters.

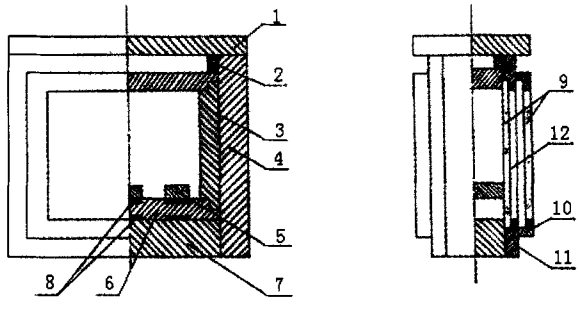

Fig.2 Schematic diagram of rectangular cavity

Two sets of two layers of glass 9 of 5 mm thickness were installed on the front and rear sides of the test cell to form windows. This window allowed for visual and photographic observation of melting zone. The air gap between the two layers of glass reduced heat loss of the test cell to the ambient. A special electric heater 12 was formed by coating a layer of transparent electrically conducting material on the glass. This heater was only used at the beginning of the experiment in order to

separate the PCM from the glass, which was necessary for achieving contact melting. During a typical experiment, the whole test cell was well insulated except when a photograph is to be taken, at which time the front and rear insulation was momentarily removed.

Research grade n-octadecane with purity≥99% was used as the phase change material for the current investigation. This PCM is desirable because its melting temperature is near the ambient temperature. As a result, the heat losses to environment is little. In addition, its liquid phase is transparent and this allows for the photographic observations. The thermophysical properties of this PCM were given below:

melting temperature: T_m=28℃
latent heat of phase change: L=244 kJ/kg
solid phase density: ρ_s=814 kg/m^3
solid phase specific heat: c_{ps}=2.15 kJ/(kg·℃)
solid phase thermal conductivity: k_s=0.358 W/(m·℃)
liquid phase density: ρ_l=793-0.52·T kg/m^3
liquid phase specific heat: c_{pl}=2.18 kJ/(kg·℃)
liquid phase thermal conductivity: k_l=0.152 W/(m·℃)
liquid phase dynamic viscosity: μ=3.9×10^{-3} kg/(m·s)
thermal coefficient of expansion: β=8.5×10^{-4} (1/℃)
Prandtl number: Pr=55.9

Because the influence parameters on the contact melting heat transfer include the Stefan number, Rayleigh number, subcooling parameters and the aspect ratio of PCM, the test run arrangement was shown in Table 1.

Table 1 Test run arrangement

Run	*Ste*	*Ra* (×10^{-8})	S_c	AR
1	1.05	6.04	0.02	0.54
2	2.10	10.48	0.02	0.52
3	3.15	15.72	0.02	0.52
4	1.05	6.04	0.03	0.54
5	2.10	12.08	0.03	0.54
6	3.15	16.50	0.03	0.53
7	1.05	5.77	0.04	0.53
8	2.10	11.00	0.04	0.53
9	3.15	16.50	0.04	0.53
10	1.05	2.75	0.02	0.42
11	3.15	8.25	0.02	0.42
12	1.05	2.75	0.03	0.42
13	3.15	8.25	0.03	0.42
14	1.05	2.43	0.04	0.40
15	3.15	6.85	0.04	0.40

Because liquid paraffin has a high dissolving capacity for air, the preparation for each test began with the degasification of the phase change material. For this purpose, the PCM underwent a solidification and melting cycle under vacuum and was then carefully siphoned into the test cell while its temperature was well above the melting point. To prevent the formation of internal voids, only a 10 mm depth of the PCM was siphoned into the cavity; it was then solidified by circulating cold water through the two vertical wall of the test cell. Another 10 mm of the melted PCM was siphoned to the cavity and solidified, and the process was repeated until the total height of PCM in the test cell reached the prescribed one.

Uncertainty Analysis

Heat power was determined by means of measuring the voltage and resistance. Voltage V was measured by a PZ12a-type digital voltmeter with an uncertainty of 1.2%. Resistance R was measured by an electric bridge with a maximum uncertainty of 0.35%. Therefore, the uncertainty in measuring power is

$$\frac{\delta P}{P}=2\frac{\delta V}{V}+\frac{\delta R}{R}=0.75\%$$

The maximum uncertainty of temperature measurement (including the uncertainty of data acquisition system) is ±0.2℃, and the lowest temperature measured in the present study was 23℃, so the overall uncertainty of temperature measurement is 0.8%.

The resolution of the image processing system is 256 ×256, and the smallest aspect ratio AR in the present paper was 0.392, so the maximum uncertainty of measuring the total area is

$$\frac{\delta V_0}{V_0}=\frac{1}{256}+\frac{1}{256\cdot AR}=1.39\%$$

Since the minimum solid phase fraction measured was 32%, the maximum deviation in determining the area of the solid phase is

$$\frac{\delta V_s}{V_s}=\frac{1}{256}+\frac{1}{256\cdot AR\cdot(V_s/V_0)}=3.5\%$$

Thus, the uncertainty in determining the melt fraction is

$$\frac{\delta(V/V_0)}{V/V_0}=2\frac{\delta V_s}{V_s}+\frac{\delta V_0}{V_0}=4.89\%$$

Uncertainty in measuring time is negligible.

Results and Discussion

Solid-liquid interface shapes

Typical progression of the solid-liquid interface with time, traced directly from the photographs, was shown in Fig.3. At early stage, the three-melt zones seemed to be smooth and regular, which indicated that the conduction was the dominant mode of heat transfer. As melting continued, natural convection began in the liquid phase, as was indicated by the appearance of a non-uniform melt region shown in Fig.3(b). Because the melted liquid

took up the space between the solid-liquid interface and the heat source surface, the foregoing process was a fixed melting process. Later on, the remainder PCM between heat sources become less and less. As a result, the block solid PCM dropped and contact melting began. The similar process, in which fixed melting and contact melting take place alternatively, was observed in the subsequent process.

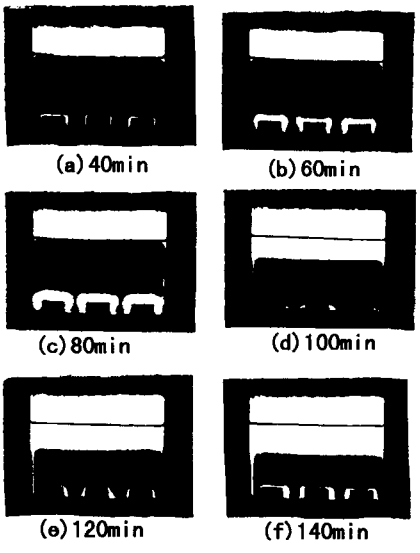

Fig.3 Solid-liquid interface (Run 9)

Surface temperatures of discrete heat sources

Surface temperature variation of discrete heat sources as a function of time were shown in Fig.4~6. At early stage of the melting process, the upper surface temperatures of the three discrete heat sources were nearly the same. After this stage, the surface temperatures increased gradually with time and eventually achieve its peak value. Thereafter, natural convection began to play a role in the melting of PCM, so there might be a little drop in surface temperature. As time progressed, the natural convection predominated. As a result, the surface temperatures of the three heat sources reached a steady value. After a certain period of time, the surface temperatures of the heat sources decreased rapidly with increasing time. This corresponds to the stage of contact melting.

The effect of Stefan number on the surface temperature of heat sources is presented in Fig.4. As can be seen, the larger the Stefan number, the more rapid the melting process and the more frequently the contact melting occurs. The maximum surface temperature of the heater in the case of large Stefan number was higher than in the case of small Stefan number.

Fig.5 shows the effect of initial subcooling on the surface temperature of heat sources. Evidently, the initial subcooling can play a significant role only in early stage of the melting process. Its influence on the melting of PCM disappeared after the fixed melting entered the quasi-steady state.

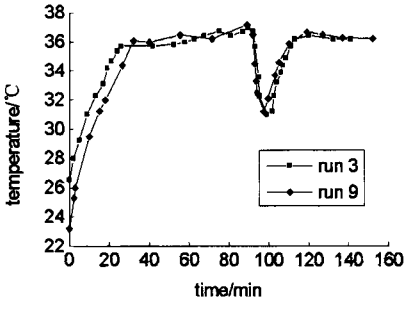

Fig.5 Effect of initial subcooling on the surface temperature of heat source

The effect of the aspect ratio of PCM on the surface temperature of heat sources is illustrated in Fig.6. The smaller the aspect ratio, the earlier the contact melting may take place and therefore, the more frequently the contact melting takes place.

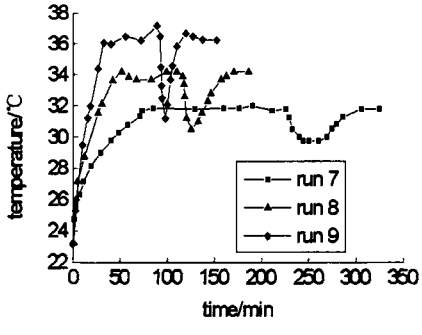

Fig.4 Effect of Stefan number on the surface temperature of heat surface

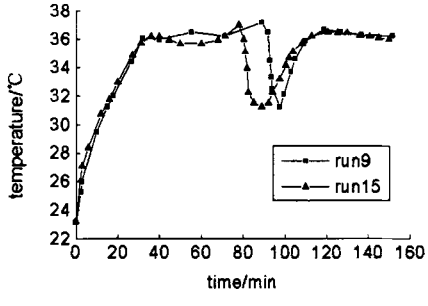

Fig.6 Effect of aspect ratio of PCM on the surface temperature so heat source

Melt Fraction

The melt fraction is defined as the ratio of the volume occupied by the liquid phase to the total volume of the PCM and is determined by the aforementioned image processing system. The variations of melt fraction with time, as well as the effect of the Stefan number on melt fraction, are illustrated in Fig.7. Linear relationships were observed for various operating conditions. This can be attributed to the constant flux of heat transfer. In addition, the larger the Stefan number, the more rapidly the melt fraction increases with time.

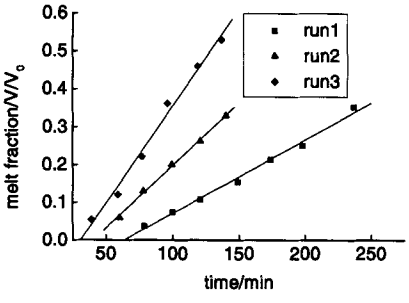

Fig.7 Effect of *Ste* number on melt fraction

The effect of initial subcooling on melt fraction is shown in Fig.8. For two different initial subcooling parameters, the two lines connecting the data points are closely parallel to each other. Accordingly, the existence of initial subcooling do not change the rate of the melt fraction rise with time, but postpone the melting process, more exactly, the first fixed melting process, to some later time.

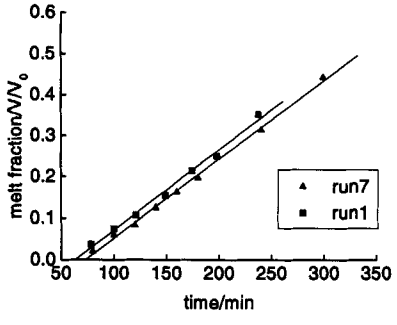

Fig.8 Effect of initial subcooling on melt fraction

The influence of aspect ratio of PCM on melt fraction was also studied (shown in Fig.9). The Stefan number and initial subcooling parameters in these two cases are the same, but the aspect ratio remains different. Evidently, the rate of the melt fraction rise with time for the case of low AR value is much slower than that for the case of high AR value.

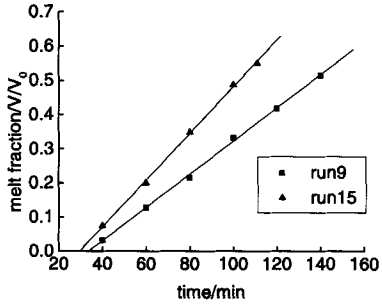

Fig.9 Effect of aspect ratio of PCM on melt fraction

Conclusions

This paper described an intermittent contact melting occurred in a rectangular enclosure heated below with local heat sources. The melting process is affected by various parameters. The larger the Stefan number and the aspect ratio of PCM, the more rapidly the melting proceeds and the more frequently the contact melting occurs. The effect of the initial subcooling on melting process does exist only in the very early stage and will disappear after the melting process enters the contact melting stage.

The present work extended the earlier investigation on the melting process in a rectangular cavity. The detailed data given in the present paper can be used as a benchmark for evaluating new numerical simulation techniques in this field.

References

[1] R Viskanta. Phase Change Heat Transfer. In Solar Heat Storage: Latent Heat Material (edited by G.A.Lane), CRC Press, Boca Raton, Florida, 1983

[2] C J Ho, R Viskanta. Heat Transfer during Melting from an Isothermal Vertical Wall. ASME J. Heat Transfer, 1984, 106(1): 12−19

[3] M Bareiss, H Beer. Experimental Investigation of Melting Heat Transfer with Regard to Different Geometric Arrangements. Int. Comm. Heat Mass Transfer, 1984, 11: 323−333

[4] D Nicholas, Y Bayazitoglu. Heat Transfer and Melting Front within a Horizontal Cylinder. J. Solar Energy Engineering, 1980, 102: 229−232

[5] M K Moallemi, R Viskanta. Melting around a Migrating Heat Source. ASME J. Heat Transfer, 1985, 107(2): 451−459

[6] E M Sparrow, S V Patankar, S Ramadhyani. Analysis of Melting in the Presence of Natural Convection in the

Melt Region. ASME J. Heat Transfer, 1977, 99: 520—526

[7] A J Fowler, A Bejan. Contact Melting during Sliding on Ice. Int. J. Heat Mass Transfer, 1993, 36(5): 1171—1179

[8] Zhou Jianhua, Chen Mingyong, Chen Zhongqi. Study on the Freezing of PCM in Annular Space. Chinese Journal of Computer Physics, 1996, 13(4): 481—488

[9] C Gau, R Viskanta. Melting and Solidification of a Metal System in a Rectangular Cavity. Int. J. Heat Mass Transfer, 1984, 27(1): 113—123

[10] Zhang Yuwen, Chen Zhongqi, Wang Qijie, et al. Melting in an Enclosure with Discrete Heating at a Constant Rate. Experimental Thermal and Fluid Science, 1993, 16(2): 196—201

[11] Y Wang, A Amiri, K Vafai. An Experimental Investigation of the Melting Process in Rectangular Enclosure. Int. J. Heat Mass Transfer, 1999, 42: 3659—3672

[12] A A Sarmarskii, P N Vabishchevich, O P Iliev, et al. Numerical Simulation of Convection/Diffusion Phase Change Problems — A Review. Int. J. Heat Mass Transfer, 1993, 36(17): 4095—4106

[13] V R Voller. An Overview of Numerical Methods for Solving Phase Change Problems. In Advances in Numerical Heat Transfer, edited by W J Minkowycz, E M Sparrow, Washington, D C: Taylor & Francis, 1997, 1: 341—380

(*continued from page* 288)

References

[1] Wang Aijun. Investigation on Mechanism of Steam Reactivation of Lime for CFB Flue Gas Desulfurization: [Doctor Thesis]. Beijing: Tsinghua University, 2000

[2] Sauer H, Anders R. Operating Experience with a Dry FGD Plant Using a CFB at the Brown Coal-Fired Power Station in Borken. Research Report of Lurgi GmbH, Germany, 1989

[3] Fan Baoguo. Experimental Study on the Flue Gas Desulphurization by a Circulating Fluidized Bed: [Master Thesis]. Beijing: Tsinghua University, 1996

[4] Wu Yongsheng, Fang Keren. Measurement of Thermal Parameters. Beijing: Electrical Power Industry Press, 1981. 154

[5] Liu Tianqi, Liu Zengkai, Zhang Xiguang, et al. The Handbook of the Atmosphere Pollution Control. Shanghai: Shanghai Science and Technology Press, 1987, 284